# Nitrous oxide production, mechanisms, and modeling from a denitrifying phosphorus removal bioreactor

McKenna Farmer[1], Fabrizio Sabba[2], George Wells[1*]
1 Civil and Environmental Engineering, Northwestern University, Evanston, IL, USA
2 Black & Veatch, Overland Park, KS, USA
*corresponding author: george.wells@northwestern.edu

## Abstract

Nitrous oxide ($N_2O$) is a potent greenhouse gas produced as an unintentional, undesired byproduct in many nitrogen removal bioprocesses. Given the considerable challenges in managing $N_2O$ emissions from wastewater treatment, $N_2O$ could be reframed as a value-added product if intentionally generated and captured. This study assesses $N_2O$ production and mechanisms in a Coupled Aerobic-anoxic Nitrous Decomposition Operation with Phosphorus removal (CANDO+P) reactor. Optimal performance was achieved when the reactor was fed with a mixture of propionate and glucose, resulting in $N_2O$ was production up to 50% of influent nitrogen. Through 16S rRNA amplicon and shotgun metagenomic sequencing, we found that *Candidatus* Accumulibacter were the dominant phosphorus accumulating organism (PAO). Assembly of a high-quality metagenome-assembled genome showed that *Ca.* Accumulibacter encoded a full complete denitrification pathway from nitrite to nitrogen gas. We also found abundant populations of denitrifying glycogen accumulating organisms (GAO) and ordinary heterotrophic organisms (OHO). We also incorporated truncated denitrification pathways into a process model to predict $N_2O$ generation. $N_2O$ predictions were the most similar to observed results when the denitrification pathways of PAO, GAO, and OHO model populations reflected denitrification gene abundances from the metagenomic sequencing analysis. Our work demonstrates the feasibility of using non-VFA carbon for intentional $N_2O$ generation and

28 provides broader insights into $N_2O$ generation and truncated denitrification pathways of

29 denitrifying PAO and GAO.

30

## 1. Introduction

Nitrous oxide ($N_2O$) is a greenhouse gas with approximately 300 times the global warming potential of carbon dioxide ($CO_2$). $N_2O$ can constitute a majority of greenhouse gas emissions from wastewater treatment plants (Daelman et al., 2013), and $N_2O$ emissions from domestic wastewater treatment represent ~5% of $N_2O$ emissions in the US (EPA, 2024). Reducing $N_2O$ emissions is an obvious target for reducing the carbon footprint of wastewater treatment, and significant research efforts are underway in pursuit of this goal. However, mitigating $N_2O$ emissions can be challenging due to competing operational goals. For example, reducing aeration is a common method to decrease energy consumption, thereby decreasing the carbon footprint of the process, but low dissolved oxygen conditions may lead to nitrifier-driven $N_2O$ production (Peng et al., 2015). Shortcut nitrogen removal methods such as nitritation-denitritation processes can also unintentionally increase $N_2O$ production due elevated nitrite ($NO_2^-$) concentrations (Zeng et al., 2003; Roots et al., 2020). Other factors may also increase $N_2O$ emissions besides the process configuration, including temperature (Hu et al., 2011), salinity (Shao et al., 2020), and influent carbon to nitrogen ratios (Velho et al., 2017). Given the challenges in managing $N_2O$ emissions from wastewater treatment, $N_2O$ could be reframed as a value-added product if intentionally generated and captured to prevent fugitive emissions.

$N_2O$ has a variety of uses and is a useful oxidant in combustion reactions. $N_2O$ has been used for decades in motorsports (Kelly, 2016) and has also been used as a propellant in aerospace applications (Gohardani et al., 2014; Werling et al., 2020). $N_2O$ is also being assessed for use as an oxidant in other applications, such as the production of functionalized phenols (Le Vaillant et al., 2022). Within a wastewater treatment facility, $N_2O$ gas could be used to increase power output from biogas combustion (Scherson et al., 2014). $N_2O$ gas is industrially produced

by decomposing ammonium nitrate with heat, which presents significant environmental health and safety concerns. Furthermore, ammonium nitrate is derived from Haber-Bosch, an energy intensive process of nitrogen sequestration from the atmosphere that generates 1-2% of global $CO_2$ emissions (Smith et al., 2020). Intentional $N_2O$ generation, capture, and combustion is an opportunity to redirect this potent greenhouse gas for a useful purpose.

Intentional $N_2O$ production from wastewater has been explored in the coupled aerobic−anoxic nitrous decomposition operation (CANDO) process (Scherson et al., 2014, 2013; Weißbach et al., 2018), which produces $N_2O$ through the denitrification pathway by feeding organic carbon and nitrogen (as $NO_2^-$) separately. The CANDO+P process (Gao et al., 2017) is a further development of the process where biological phosphorus removal is also incorporated through enrichment of denitrifying phosphorus accumulating organisms (DPAO). The CANDO+P process attempts to enrich a community where $N_2O$ reduction is minimized, while the preceding steps of the denitrification pathway are maintained such that $N_2O$ is the primary denitrification product. Like many other denitrifiers, DPAO and denitrifying glycogen accumulating organisms (DGAO) may possess incomplete denitrification pathways which are highly specific by species and strain (Albertsen et al., 2016; Petriglieri et al., 2022; Stewart et al., 2024). In general, the presence of $NO_2^-$ as an electron acceptor, alone or paired with other oxidized nitrogen species, increases $N_2O$ accumulation in DPAO and DGAO (Marques et al., 2018). Previous work in our lab on a CANDO+P system has found that different denitrifying populations in the same culture (DPAO, DGAO, and non-PAO/GAO denitrifiers) differentially expressed denitrification genes, resulting in a highly modular denitrification process where $NO_2^-$ reductases were also expressed at a higher level than $N_2O$ reductases (Wang et al., 2021). Similar results have been observed in a biological phosphorus removal system not intended for $N_2O$

77 production Vieira et al. (2018) as well as in other environmental contexts like soils (Bru et al.,
78 2011; Nadeau et al., 2019).

79 The goals of this work are to (1) demonstrate CANDO+P for $N_2O$ accumulation on low
80 COD:N wastewater with non-VFA carbon (2) understand distribution of denitrifying genes in the
81 community and (3) predict $N_2O$ production through process models informed by molecular data.
82 The results of this work are expected to increase our ability to optimize $N_2O$ accumulation by
83 DPAO for resource recovery and can also be considered in the broader context of understanding
84 $N_2O$ emissions from nutrient removal bioprocesses.

85 **2. Results and Discussion**

86 **2.1. Reactor performance and $N_2O$ production on glucose-amended feed**

87 The reactor was adapted for orthoP removal by approximately day 50 of operation (SI
88 Figure 1). However, orthoP removal performance became unstable around day 110 and continued
89 throughout the rest of the phase. This deterioration of performance seems to have coincided with
90 changes in the microbial community, which is described further in section 2.2. Given the reactor
91 instability, the COD:P ratio was increased to encourage PAO growth in Phase II. However, this
92 change did not improve orthoP removal, and in a majority of sampling points, no net orthoP
93 removal was achieved. $NO_2^-$ removal was consistent during this phase (average of 92 ± 16%),
94 suggesting that conventional denitrifiers or DGAO were active during this phase rather than
95 DPAO. During this phase, $N_2O$ accumulation was also observed during some anoxic phases but
96 inconsistently and at low concentrations (<1 mgN/L).

97 Phase III (days 484-512) was used as a transition period to move the reactor from VFA-
98 only to a mixed carbon feed. Previous work has demonstrated that PAO grown on acetate may
99 have greater carbon uptake ability than GAO when the feed is switched to propionate (Oehmen

et al., 2005), therefore the influent feed was amended with propionate on day 484 in a 1:1 COD ratio with acetate for a final concentration of 300 mg/L COD. During this phase, preferential uptake of propionate was observed, and acetate was carried over between cycles (SI Figure 2). $NO_2^-$ removal was consistent during this phase (average of 94 ± 10%), and $N_2O$ accumulation began to occur consistently, with peak values around 1 mgN/L, representing 5-10% conversion of influent $NO_2^-$-N.

Phase IV (days 512-750) was started by modifying the COD source to propionate and glucose on day 512 in a 2:1 COD ratio with an initial concentration of 250 mg/L COD. A typical in-cycle profile is shown in Figure 1. Unlike Phase III, there was no COD carry over between cycles, and COD was consumed completely within the anaerobic phase. During the initial part of the phase, there was a clear substrate preference for glucose over propionate (SI Figure 3). Rapid COD uptake was observed during this phase, so the anaerobic phase length was reduced from approximately 1.6 hours to 0.6 hours to prevent endogenous respiration, and the COD was reduced to 100 mg/L with a 1:1 propionate to glucose ratio on day 688. During Phase IV, orthoP removal was highly variable, reaching a maximum removal of 90%, but having a net negative average removal and large standard deviation (-34 ± 62%). In most cycles, we observed both anoxic and aerobic orthoP uptake (SI Figure 5). The mixed propionate and glucose feed resulted in $NO_2^-$ removal of 90 ± 14%, within the range of previous phases. As expected, the COD:N ratio had a strong, positive correlation with the anoxic orthoP uptake and $NO_2^-$ reduction rate (SI Figure 5). The ranges of anoxic orthoP uptake and $NO_2^-$ reduction were within ranges previously observed in a CANDO+P reactor (Gao et al., 2020). This phase had more consistent $N_2O$ accumulation than the previous phases, between 10-30% of the influent $NO_2^-$-N (SI Figure 4) and up to 50% during some cycles. The maximum specific $N_2O$ production rate was 0.96 ± 0.36

123 mg$N_2O$-N/gTSS/h. Overall, the addition of glucose to the COD feed improved the consistency of
124 $N_2O$ production but did not offer vast improvements to the orthoP removal performance.

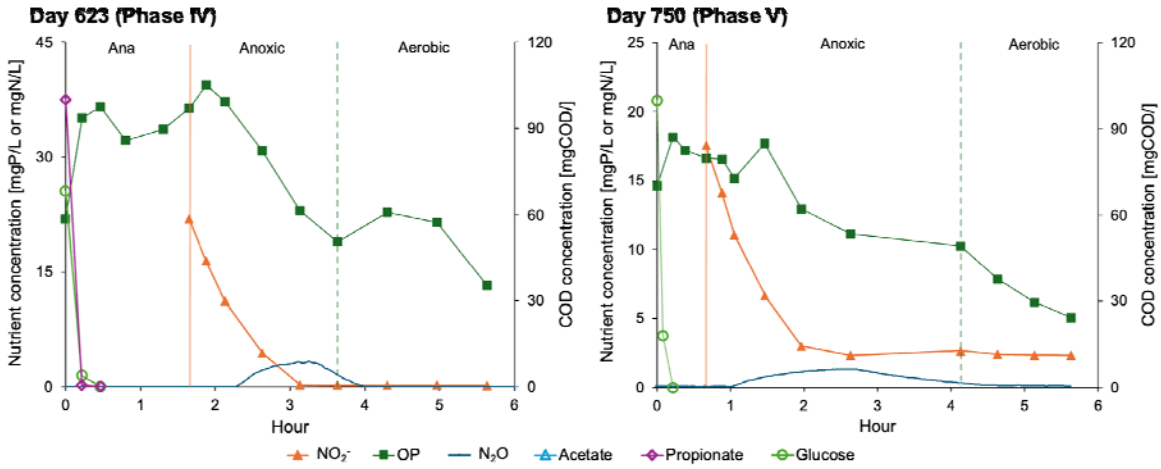


125
126 **Figure 1 Representative in-cycle nutrient and carbon profile from days 623 and 720.**

127 In the final operational phase (Phase V), the COD feed was switched to glucose only to
128 test the viability of CANDO+P on non-VFA carbon. On the first day of glucose-only operation
129 (day 720), denitrification was not complete (Figure 1), suggesting that the propionate dosed in
130 Phase IV provided important benefits to carbon storage products used for denitrification. In this
131 phase, we observed a shift from unstable phosphorus removal to more robust performance. In the
132 first month of the phase, the effluent orthoP was the same as or higher than the influent, and the
133 orthoP removal averaged over the whole phase was highly variable (average of 32 ± 54%).
134 However, towards the end of the phase, effluent orthoP reached the detection limit (0.02 mgP/L,
135 ~99% removal efficiency). $N_2O$ accumulation occurred during this phase but was lower in
136 magnitude and rate than Phase IV. Influent $NO_2$-N was gradually increased up to 30 mgN/L in
137 this phase, but peak $N_2O$ values were between 1-2 mgN/L, representing only up to 6%
138 conversion of influent $NO_2$-N, with a maximum observed $N_2O$ production rate of 0.25 mg$N_2O$-
139 N/gVSS/h. Although the glucose-only feed provided an improvement to orthoP removal
140 performance, this COD source resulted in lower $N_2O$ production on its own compared to the

previous phase with VFA and glucose. While detrimental for our goal of $N_2O$ production, this result has positive implications for processes fed with significant quantities of glucose or possibly other simple sugars where $N_2O$ production is undesirable.

While the CANDO+P reactor in this work achieved consistent $N_2O$ production in Phases IV and V with glucose as a COD source, the $N_2O$ production was lower than previous studies. For example, Gao et al. (2017) achieved an $N_2O$ conversion efficiency of 70% of influent $NO_2^-$-N compared to up to the typical value of 30% and maximum value of 50% achieved in this work. The $N_2O$ production rate of 0.96 ± 0.36 mg$N_2O$-N/gVSS/h in Phase IV was also much lower than previous values on acetate-only (5.7 ± 2.0 mg$N_2O$−N/gVSS/h) and propionate-only (4.9 ± 2.1 mg$N_2O$−N/gVSS/h) observed by Gao et al. (2017). However, the $N_2O$ production rate observed here was consistent with observations from a pilot fed with real wastewater with a rate of 1.30 ± 0.20 mg$N_2O$−N/gVSS/h (Weißbach et al., 2018). A CANDO reactor was also recently operated with conversions near 100% in some cycles (Wang et al., 2020), much higher than achieved here, but Wang and colleagues also observed cycles where complete $N_2O$ was produced and completely reduced before the end of the anoxic phase, similar to what we observed in Phase IV and V of this study. To better understand the microbial drivers of $N_2O$ production in this reactor, we next turned to a suite of complementary molecular microbial community analyses.

### 2.2. Denitrifying community shifts over the reactor operation

16S rRNA amplicon sequencing was used to identify prevalent PAO, GAO, and denitrifier taxa in the reactor. Relative abundances from 16S rRNA sequencing for the whole study are shown in Figure 2. As previously mentioned, orthoP removal performance in Phase I was unstable after an increase in the $NO_2^-$ dose. The only PAO detected in Phase I, *Ca.* Accumulibacter, increased in abundance until approximately day 125 but tapered off and

eventually declined over the rest of the phase. On the other hand, the relative abundance of the GAO *Plasticicumulans* increased, reaching its peak around day 150, when orthoP instability was greatest. *Plasticicumulans* are in the *Competibacteraceae* family and are generally considered GAO due to their uptake of soluble COD under feast-famine conditions (McIlroy et al., 2014). These organisms do not have denitrification capabilities (Tamis et al., 2014), so denitrification was likely carried out by other organisms during this unstable period, potentially *Dechloromonas* which increased in abundance after day 125. Some species of *Dechloromonas* possess the polyphosphate accumulating metabolism, but these species were not detected in Phase I. Another denitrifier present during Phase I was *Flavobacterium,* which have previously been associated with other nitrite-fed phosphorus removal bioreactors (Lv et al., 2014; Wang et al., 2024). Overall, the decline of *Ca.* Accumulibacter PAO and concurrent GAO and denitrifier community shifts likely contributed to the poor orthoP removal performance during Phase I.

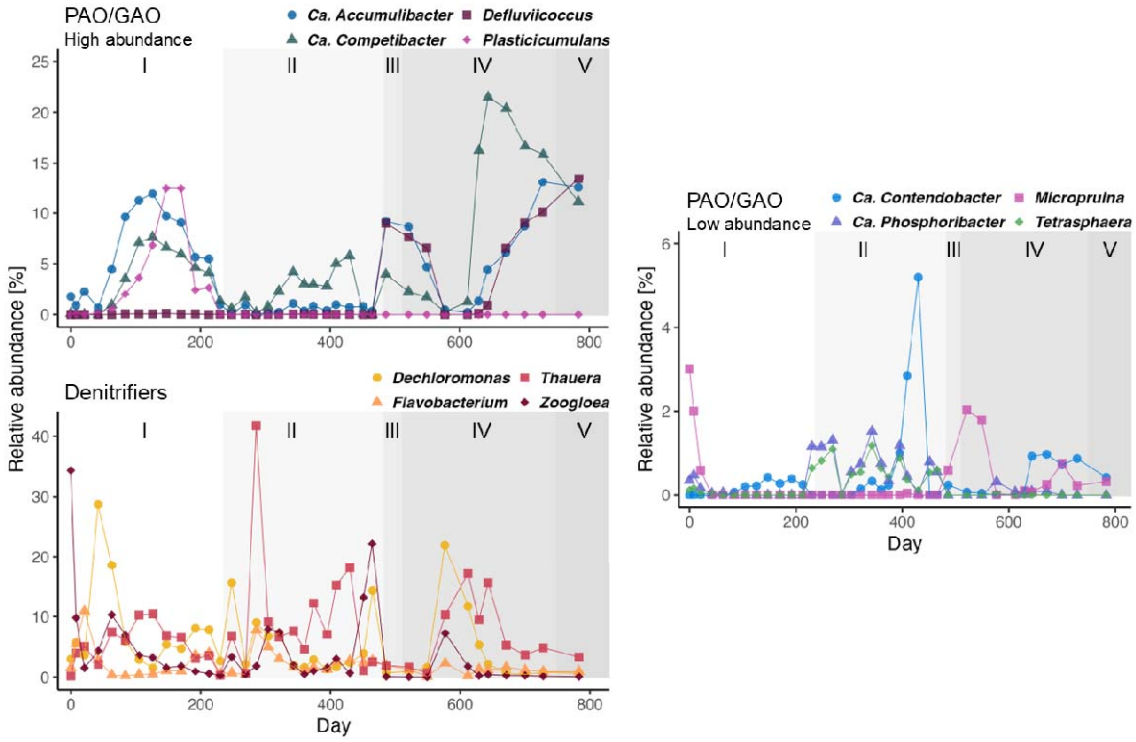


**Figure 2 PAO, GAO, and denitrifier relative abundances from 16S rRNA sequencing. Phases (I-V) are denoted by the shaded areas.**

During Phase II (acetate and high $NO_2^-$ feed), which had largely unstable orthoP removal, *Ca.* Accumulibacter abundance dropped to a median of 0.4% compared to 5.5% in Phase I. In place of *Ca.* Accumulibacter, the PAO *Ca.* Phosphoribacter and *Tetrasphaera* increased in relative abundance, though not to the same magnitude as *Ca.* Accumulibacter (Figure 2). These organisms were present in the seed sludge but had been at negligible abundances throughout Phase I. Similarly, the GAO *Ca.* Contendobacter was present during Phase I but had a greater abundance in Phase II and a notable spike around day 400. The GAO *Plasticicumulans* did not reemerge in this phase or subsequent phases.

The transitional Phase III (acetate and propionate feed) corresponded to an increase in *Ca.* Accumulibacter, as well as the GAO *Ca.* Competibacter and *Defluviicoccus.* The sudden enrichment of *Defluviicoccus* may have been related to the addition of propionate, as previous work has demonstrated that *Defluviicoccus* will uptake propionate even in the presence of other substrates like acetate (Burow et al., 2007). *Defluviicoccus* has also been observed at high abundances in other denitrification systems with significant $NO_2^-$ concentrations, including a CANDO system (Wang et al., 2020) and a partial-denitrification anammox system (Chu et al., 2021), though other works show *Defluviicoccus* suppressed in the presence of $NO_2^-$ (Tayà et al., 2013).

In Phase IV (propionate and glucose feed), PAO and GAO abundances decreased initially, then rebounded after approximately 60 days. Notably, we documented a strong positive correlation between *Ca.* Accumulibacter and *Defluviicoccus*, which had a Pearson correlation of 0.94 ($p < 0.001$). A correlation is reasonable given the suitability of feast-famine feeding for both of these organisms, but the strength of the correlation and nearly identical abundances was surprising. Another notable feature was the rapid increase in *Ca.* Competibacter in Phase IV,

which was driven by two strains of *Ca*. Competibacter that were not highly abundant prior to day 600 (SI Figure 6). Additionally, the GAO *Micropruina* also increased in abundance at the beginning of the phase. *Micropruina* can directly uptake glucose under anaerobic conditions (McIlroy et al., 2018), giving them a competitive advantage for carbon uptake in this phase. Overall, the net abundances of GAO were much greater than PAO in Phase IV and V, which may have contributed to the inconsistent orthoP removal performance observed in this time period.

### 2.3. Microbial community features driving $N_2O$ accumulation

Shotgun metagenomic sequencing was used to understand denitrifying capabilities of the microbial community. Metagenomic samples were collected primarily during Phase IV. In this phase, a mix of propionate and glucose were added to the feed, and $N_2O$ was produced then mostly reduced by the end of the anoxic phase. The sequencing data was first analyzed using a pathway-focused metagenomics approach for denitrification pathway genes by annotating coding sequences from contigs. Figure 3summarizes taxa relative abundances and *nosZ* gene abundances during a period of Phase IV when $N_2O$ production decreased. A notable feature is the prevalence of *nosZ* associated with *Ca.* Accumulibacter, while *nosZ* associated with other taxa decreased. *Thauera* and *Ca*. Competibacter abundances increased based on 16S rRNA sequencing, but there was a net decrease in *Thauera*-associated *nosZ* and no increase in *Ca.* Competibacter-associated *nosZ* over the same time period. These results suggest that *Ca.* Accumulibacter contributed to $N_2O$ reduction more so than other community members, though we did not measure gene expression so cannot say definitively.

$NO_2^-$ reduction was a common function across almost all analyzed taxa (SI Figure 7), though with some variances in the specific corresponding functional gene. The genes *nirA* and *nirBD* encode assimilatory $NO_2^-$ reduction (i.e. $NO_2^-$ reduced to $NH_3$ for incorporation into

biomass) while *nirS* and *nirK* encode dissimilatory $NO_2^-$ reduction (i.e. respiration). *Defluviicoccus* was the exception to this, as the only *Defluviicoccus*-associated denitrification genes detected (*norBC*) encoded NO reduction and were at relatively low abundances compared to those from other organisms. This finding suggests that *Defluviicoccus*, though a dominant GAO by abundance, were not significant denitrifiers in this system. Other *norBC* genes were identified from the GAO *Ca.* Competibacter and *Ca.* Contendobacter as well as the denitrifiers *Dechloromonas, Thauera,* and *Zoogloea*. *Ca.* Accumulibacter-associated *norBC* genes increased in abundance over Phase IV unlike the denitrifier abundance, which decreased to undetectable levels by the end of the phase. In this reactor, *Ca.* Accumulibacter putatively encoded genomic capability for denitrification from $NO_2^-$ to $N_2$. This metagenomic analysis cannot be used to determine if the genes were all present in one organism, so a binning approach was undertaken to recover more information about *Ca.* Accumulibacter and other denitrifying community members.

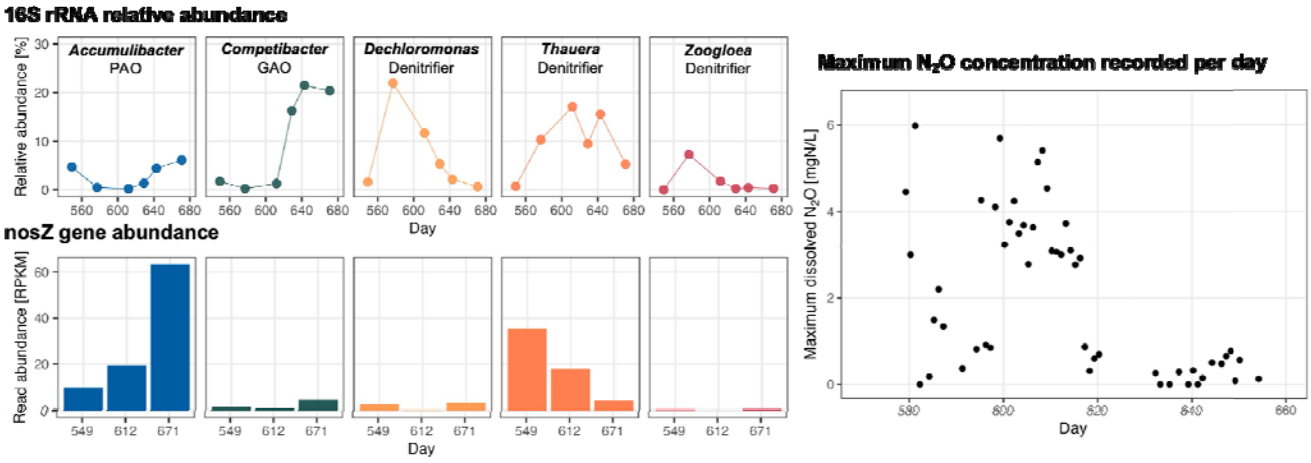


**Figure 3 Relative abundances of key PAO, GAO, and denitrifier taxa from 16S rRNA sequencing (top left), *nosZ* gene abundance from metagenomic sequencing (bottom left), and maximum $N_2O$ concentrations recorded during part of Phase IV (right).**

We employed a coupled assembly and binning approach to recover metagenome-assembled genomes (MAGs). Medium- (≥50% completeness, ≤10% contamination) and high-quality (≥90% completeness, ≤5% contamination) PAO, GAO, and denitrifier MAGs are summarized in SI Table 1, and associated denitrification genes are shown in SI Figure 8. Two *Ca.* Accumulibacter MAGs were recovered: one high-quality (CAN3.12, completeness 97.95%, contamination 1.98%) and one medium-quality (CAN_3.27, completeness 74.14%, contamination 1.72%). The *Ca.* Accumulibacter MAGs possessed genes for a complete denitrification pathway from $NO_2^-$ to $N_2$, which is in agreement with the denitrifying pathway metagenomics results. However, the NO reductase genes present in the assembled MAGs (*norV*) differed from the dominant genes in the pathway approach (*norB* and *norC*). Some *norVW* genes associated with *Ca.* Accumulibacter were detected with the pathway approach but at very low abundances (<1 RPKM).

Both *Ca.* Accumulibacter MAGs possessed *glk* genes, which encode glucokinase, an enzyme that phosphorylates glucose to glucose-6-phosphate. This molecule is an entry point for

numerous cellular functions, including glycolysis and glycogen synthesis. The presence of *glk* in the *Ca.* Accumulibacter MAGs suggests that these organisms have a direct pathway for glucose utilization. Our findings mirror a recent study which reported the direct uptake and utilization of glucose by *Ca.* Accumulibacter as well as assembly of a *Ca.* Accumulibacter MAG with the *glk* gene (Ziliani et al., 2023). It is unclear if *Ca.* Accumulibacter use glucose directly in glycogen storage, or if they can ferment glucose to pyruvate, then use this for PHA storage. In this study, we observed what appears to be a two phase orthoP release in Phase IV when propionate and glucose were dosed together, despite both carbon sources being taken up at a similar rapid rate (Figure 1). This work cannot be used to draw any definitive conclusions on the specific glucose utilization pathways by *Ca.* Accumulibacter but does show a potential for non-VFA carbon uptake and orthoP release by this canonical PAO.

### 2.4. Microbiome-informed mechanistic model

A mechanistic mathematical process model was developed to simulate $N_2O$ production during Phase IV using three denitrifying populations: DPAO, DGAO, and denitrifying OHO with internally stored carbon. Three scenarios were evaluated based on the denitrification pathway metagenomics results. The “full pathways” scenario was evaluated assuming DPAO, DGAO, and OHO performed complete reduction of $NO_2^-$ to NO to $N_2O$ to $N_2$. The “truncated DGAO” scenario was evaluated assuming complete denitrification by DPAO and OHO, and no $N_2O$ reduction by DGAO based on the low DGAO-associated *nosZ* gene abundances observed during Phase IV (Figure 3, SI Figure 7). The “truncated DGAO+OHO” scenario was evaluated assuming complete denitrification by DPAO, and truncated denitrification pathways in both DGAO and OHO based on low *nosZ* and *norBC* gene abundances in these functional groups (**Error! Reference source not found.**). Rate equations, stoichiometry, and parameter values

were based on the work of Liu et al. (2015) for DPAO, Ren et al. (2023) for DGAO, and Gujer et al. (1999) for OHO, and further details are provided in the supporting material.

$N_2O$ profile predictions compared to the observed values on day 623 are shown in Figure 4. The full pathways scenario did not predict any significant $N_2O$ accumulation, deviating the most from the observed values, and had a root mean square error (RMSE) value of 2.21. The truncated DGAO scenario predicted some $N_2O$ accumulation but was not consistent with the leading edge of the $N_2O$ profile or the overall magnitude and had an RMSE value of 1.36. The truncated DGAO+OHO scenario had the best match to the observed $N_2O$ profile in both shape and magnitude with an RMSE value of 0.68. Similar to the $N_2O$ profile, the $NO_2^-$ profile (SI Figure 10) was best captured by the truncated DGAO+OHO scenario (RMSE = 1.12), followed by the truncated DGAO (RMSE = 1.68) and full pathway (RMSE = 2.49) scenarios.

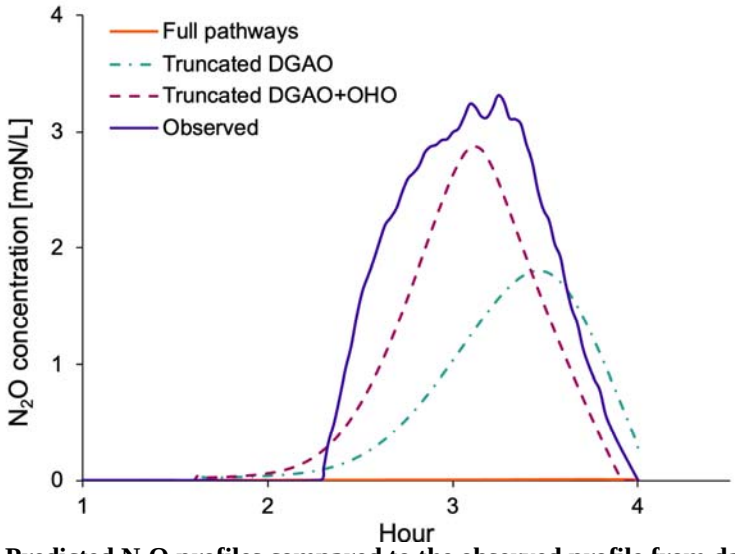


**Figure 4 Predicted $N_2O$ profiles compared to the observed profile from day 623.**

Future iterations of this model can improve the accuracy of the $N_2O$ and $NO_2^-$ profiles, potentially through incorporation of more accurate inhibition effects from $NO_2^-$. Ribera-Guardia et al. (2016) demonstrated that DGAO-enriched cultures produced more $N_2O$ than DPAO-enriched cultures when fed $NO_2^-$, likely due to a greater inhibitory effect of $NO_2^-$ on DGAO than

296 DPAO. The importance of $NO_2^-$ inhibition factors is demonstrated in this work in SI Figure 11,
297 where the truncated DGAO+OHO scenario was run assuming the same inhibition constant (8
298 $gN/m^3$) for all denitrification steps. In this scenario, the peak $N_2O$ predicted was 4.2 mgN/L
299 compared to 2.9 mgN/L in the original model, an increase of around 50%. While this model
300 could be improved through more rigorous calibration, particularly for $NO_2$ inhibition, the results
301 demonstrate the utility of incorporating full and partial denitrification pathways by multiple
302 functional groups to improve $N_2O$ predictions.

303 We also assessed the accuracy of the model in fitting the observed orthoP profile (SI
304 Figure 10). All three modeling scenarios largely captured the magnitude of orthoP release and
305 uptake. The two phase orthoP release observed in Phase IV was not captured by the model. This
306 was unsurprising as we used one state variable for soluble carbon ($S_S$) rather than individual
307 variables for glucose and propionate. Existing model structures partition carbon into different
308 categories to capture carbon availability dynamics over time, such as ASM2d which includes
309 fermentation products ($S_A$), fermentable readily biodegradable substrate ($S_F$), and slowly
310 biodegradable solids ($X_S$) (Henze et al., 1999). This type of model structure can serve as an
311 example of carbon partitioning, though in this work, it is obvious that both VFA and glucose are
312 readily biodegradable and suitable for rapid uptake. Despite this limitation of our model on
313 carbon uptake dynamics, all three scenarios performed reasonably well at predicting net orthoP
314 release and anoxic orthoP uptake.

315 Overall, our predictions for $N_2O$, $NO_2^-$, and orthoP relative to the observed data provide
316 compelling evidence that incorporating truncated denitrification pathways into process models
317 based on metagenomics data can be a useful route to predicting $N_2O$ production and
318 consumption in DPAO and DGAO enriched bioprocesses. The goal of this modeling work was

not to precisely calibrate and validate the model but rather to demonstrate the utility of this approach. Metagenomics-informed modeling has been tested with varying levels of success in soils (Graham et al., 2016; Nadeau et al., 2019) and similar approaches have been tested more recently in wastewater process modeling specifically, including modeling simplified partial denitrification ($NO_3^-$ to $NO_2^-$, $NO_2^-$ to $N_2$) of heterotrophic denitrifiers (Su et al., 2023) and nitrite oxidizing bacteria (NOB) (Sampara et al., 2022). Metagenomics-informed modeling has even been tested in a denitrifying EBPR process with mixed populations of DPAO and DGAO (Oehmen et al., 2010). The approach presented here builds upon the work of Oehmen et al. (2010) by developing the model structure from metagenomic data collected from the reactor of interest, rather than relying on metagenomic data published from other study systems. This metagenomics-informed modeling approach would need further validation for full-scale activated sludge. More complicated microbial communities and influent immigration of microbes from the conveyance system would likely dilute the signal of denitrification genes. Furthermore, there are a variety of factors besides truncated denitrification pathways in heterotrophs which impact $N_2O$ production, particularly nitrifier-derived $N_2O$ production, oxygen inhibition, and transitional conditions between redox zones (Vasilaki et al., 2019).

## 3. Conclusion

A CANDO+P reactor was operated for over two years and evaluated for performance on VFA and non-VFA carbon, denitrifying microbial community dynamics, and utility of metagenomics data for improving $N_2O$ modeling. The CANDO+P reactor had unstable performance on an acetate-only feed, possibly due to an overabundance of the GAO *Plasticiculumans*. $N_2O$ production rate and reliability improved when the propionate feed was supplemented with glucose in Phase IV, reaching up to 50% conversion of influent nitrogen with

a production rate of 0.96 ± 0.36 mg$N_2O$-N/gVSS/h. This production was significantly higher than typical denitrification processes but fell short of previous CANDO/CANDO+P studies. Microbial community analysis via 16S rRNA sequencing showed that *Ca.* Accumulibacter were the dominant PAO throughout the study, and while GAO *Ca.* Competibacter and *Defluviicoccus* were also persistent throughout the reactor operation. Denitrification pathway analysis via shotgun metagenomic sequencing provided evidence that *Ca.* Accumulibacter populations may have encoded a complete denitrification pathway from $NO_2^-$ to $N_2$ while GAO had low and nondetectable abundances of *nosZ*. A denitrification model with three denitrifying populations (DPAO, DGAO, OHO) was developed that incorporated truncated denitrification pathways based on the metagenomic sequencing data. The models with truncated denitrification pathways informed by metagenomic sequencing improved $N_2O$ predictions over scenarios assuming full denitrification pathways. This work demonstrates combined $N_2O$ production and orthoP removal through the CANDO+P process on non-VFA carbon, provides broader insights into truncated denitrification pathways of denitrifying PAO and GAO, and proposes metagenomic-informed modeling to improve predictions of $N_2O$ generation.

## 4. Materials and Methods

### 4.1. Reactor operation and conditions

A 12 L reactor was seeded with biomass from Stickney Water Reclamation Plant in May 2021 and operated for 830 days. The reactor was operated to select for DPAO through the primary react phases: fill and anaerobic react, nitrite ($NO_2^-$) dose and anoxic react, and aerobic react followed by settling and decanting. $NO_2^-$ was used as the nitrogen source to simulate effluent from an upstream nitritation reactor. The SBR was controlled using ChronTrol XT 4 circuit programmable timers. Complete SBR cycles were 8 hours, and the reactor decanted 6 L

each cycle. Synthetic wastewater was used in this work and is detailed in the supplementary information. The phases of reactor operation were based on the COD source, COD concentration, and $NO_2^-$ dose (Table 4-1). Phase I was designated as the start-up phase but was operated longer than expected due to performance upsets. The mixed liquor suspended solids (MLSS) was an average of 0.76 ± 0.30 g/L during Phases I and II and increased to an average of 5.1 ± 2.1 g/L from Phase III until the end of the study.

**Table 4-1 Reactor operational phases**

| Phase | Day | COD source | COD [mgCOD/L] | $NO_2^-$ [mgN/L] | $PO_4^{3-}$ [mgP/L] |
|---|---|---|---|---|---|
| I | 0 | Acetate | 130 | 5-10 | 21 |
| II | 237 | Acetate | 100-150 | 10-30 | 10-15 |
| III | 484 | Acetate, Propionate | 300 | 15 | 10 |
| IV | 512 | Propionate, Glucose | 90-250 | 15 | 10 |
| V | 750 | Glucose | 90-100 | 15-30 | 10 |

## 4.2. Water quality and reactor performance measurements

Reactor effluent samples were collected 2-3 times per week and measured for total and soluble chemical oxygen demand (COD), orthoP, $NO_x$ ($NO_3^-$ + $NO_2^-$), and $NO_2^-$ per APHA standard methods (APHA, 2017). Nutrient measurements were conducted on a Skalar San++ continuous flow analyzer. Reactor solids samples were collected 1-2 times per week for total suspended solids (TSS) and volatile suspended solids (VSS) measurement per APHA standard methods. Dissolved $N_2O$ concentrations were monitored with a Unisense $N_2O$ Wastewater System. High time resolution in-cycle tests were conducted approximately every week to measure soluble orthoP, $NO_2^-$, volatile fatty acids (VFA), and glucose over the course of a reactor cycle. VFA measurements for acetate and propionate were performed on a GC-FID following APHA standard methods. Soluble glucose concentrations were measured with Sigma-Aldrich and Thermo-Fisher hexokinase measurement kits following manufacturer protocols.

### 4.3. Molecular sampling and DNA sequencing

Biomass was archived weekly in 3-4 replicates for DNA-based analysis. 1.5 mL aliquots of biomass were centrifuged at 10,000G for 3 minutes and decanted, and samples were resuspended with 1 mL of tris-EDTA buffer. The samples were centrifuged and decanted again, then pellets were stored at -80ºC until further processing. DNA was extracted with the FastDNA SPIN Kit for Soil (MP Biomedicals) following the manufacturer protocol.

PCR amplification was performed on extracted DNA to amplify the V4-V5 region of the 16S rRNA gene using 515F/926R primers (Parada et al., 2016). PCR details are in the supporting information. PCR products were sent to Rush University Genomics and Microbiome Core Facility (Chicago, IL) for barcoding via second stage PCR and 2x300 bp sequencing with an Illumina MiSeq using V3 chemistry. Raw sequencing reads were processed using QIIME2, and amplicon sequence variants (ASV) were produced using deblur2. Taxonomy was assigned using the MiDAS v5.3 database (Dueholm et al., 2024).

Extracted DNA from Phases III and IV (days 451, 521, 549, 612, 671, 728) was sent to either Northwestern University NUSeq Core or SeqCenter (Pittsburgh, PA) for shotgun metagenomic sequencing. Library preparation was performed at both facilities with the Illumina DNA Prep kits following manufacturer protocols. Sequencing at the NUSeq Core was performed on a NovaSeq 6000 to generate 2x150 bp reads. Sequencing at SeqCenter was performed on a NovaSeq X Plus to generate 2x151 bp reads. Metagenomic analysis was performed on the Quest High Performance Computing Cluster at Northwestern University. Denitrification pathway analysis was performed by read trimming with fastp, assembly with MEGAHIT, prediction of protein-coding genes with Prodigal, and alignment of coding sequences to denitrification genes from UniProtKB (accessed May 2024). Coding sequences were retained with 70% or greater

sequence identity to the reference. Metagenome-assembled genome analysis was performed on the assembled contigs from MEGAHIT, which were binned using metabat2, assigned taxonomy using GTDB-Tk, and annotated with prokka. Analysis scripts are available at https://github.com/mckfarm/cando_meta. All raw reads are available at accession PRJNA1148969.

### 4.4. Modeling $N_2O$ dynamics

Process modeling was used to understand whether predictions of $N_2O$ generation could be improved with denitrification pathway information from metagenomic sequencing. Three populations were used in the model: DPAO, DGAO, and denitrifying ordinary heterotrophic organisms (OHO). The stoichiometry, rate equations, and parameters were based on Liu et al. (2015) and Ren et al. (2023), for DPAO and DGAO, and ASM3 (Gujer et al., 1999) and Liu et al. (2015) for OHO. The reactor was modeled in AQUASIM as a single completely mixed compartment (Reichert, 1994). Each denitrifying population was modeled to perform anaerobic carbon storage, and the default modeling scenario included denitrification on $NO_2^-$, NO, and $N_2O$ for all three populations. Denitrification pathway distribution of the three populations from metagenomic data was used to generate multiple test scenarios of truncated denitrification pathways in DGAO and OHO. The stoichiometric matrix, rate equations, and parameter values are detailed in the supporting information.

## 5. Acknowledgements

McKenna Farmer and George Wells were supported in part by the Israel-U.S. Collaborative Water-Energy Research Center (CoWERC), via the Binational Industrial Research and Development Foundation (BIRD) Energy Center grant EC-15. This research was also

supported in part through the computational resources and staff contributions provided for the Quest high performance computing facility at Northwestern University which is jointly supported by the Office of the Provost, the Office for Research, and Northwestern University Information Technology.

## 6. References

Albertsen, M., McIlroy, S.J., Stokholm-Bjerregaard, M., Karst, S.M., Nielsen, P.H., 2016. "Candidatus Propionivibrio aalborgensis": A Novel Glycogen Accumulating Organism Abundant in Full-Scale Enhanced Biological Phosphorus Removal Plants. Front. Microbiol. 7. https://doi.org/10.3389/fmicb.2016.01033

APHA, 2017. Standard Methods for the Examination of Water and Wastewater, 23rd edition. ed. APHA, AWWA, WEF.

Bru, D., Ramette, A., Saby, N.P.A., Dequiedt, S., Ranjard, L., Jolivet, C., Arrouays, D., Philippot, L., 2011. Determinants of the distribution of nitrogen-cycling microbial communities at the landscape scale. The ISME Journal 5, 532–542. https://doi.org/10.1038/ismej.2010.130

Burow, L.C., Kong, Y., Nielsen, J.L., Blackall, L.L., Nielsen, P.H., 2007. Abundance and ecophysiology of Defluviicoccus spp., glycogen-accumulating organisms in full-scale wastewater treatment processes. Microbiology 153, 178–185. https://doi.org/10.1099/mic.0.2006/001032-0

Chu, G., Yu, D., Wang, X., Wang, Q., He, T., Zhao, J., 2021. Comparison of nitrite accumulation performance and microbial community structure in endogenous partial denitrification process with acetate and glucose served as carbon source. Bioresource Technology 320, 124405. https://doi.org/10.1016/j.biortech.2020.124405

Daelman, M.R.J., Van Voorthuizen, E.M., Van Dongen, L.G.J.M., Volcke, E.I.P., Van Loosdrecht, M.C.M., 2013. Methane and nitrous oxide emissions from municipal wastewater treatment – results from a long-term study. Water Science and Technology 67, 2350–2355. https://doi.org/10.2166/wst.2013.109

Dueholm, M.K.D., Andersen, K.S., Petersen, A.-K.C., Rudkjøbing, V., Alves, M., Bajón-Fernández, Y., Batstone, D., Butler, C., Cruz, M.C., Davidsson, Å., Erijman, L., Holliger, C., Koch, K., Kreuzinger, N., Lee, C., Lyberatos, G., Mutnuri, S., O'Flaherty, V., Oleskowicz-Popiel, P., Pokorna, D., Rajal, V., Recktenwald, M., Rodríguez, J., Saikaly, P.E., Tooker, N., Vierheilig, J., Vrieze, J.D., Wurzbacher, C., Nielsen, P.H., 2024. MiDAS 5: Global diversity of bacteria and archaea in anaerobic digesters. bioRxiv 2023.08.24.554448. https://doi.org/10.1101/2023.08.24.554448

EPA, 2024. Inventory of U.S. Greenhouse Gas Emissions and Sinks 1990-2022 (No. EPA 430-R-24-004). EPA.

Gao, H., Liu, M., Griffin, J.S., Xu, L., Xiang, D., Scherson, Y.D., Liu, W.-T., Wells, G.F., 2017. Complete Nutrient Removal Coupled to Nitrous Oxide Production as a Bioenergy Source by Denitrifying Polyphosphate-Accumulating Organisms. Environ. Sci. Technol. 51, 4531–4540. https://doi.org/10.1021/acs.est.6b04896

Gao, H., Zhao, X., Zhou, L., Sabba, F., Wells, G.F., 2020. Differential kinetics of nitrogen oxides reduction leads to elevated nitrous oxide production by a nitrite fed granular denitrifying EBPR bioreactor. Environ. Sci.: Water Res. Technol. 6, 1028–1043. https://doi.org/10.1039/C9EW00881K

Gohardani, A.S., Stanojev, J., Demairé, A., Anflo, K., Persson, M., Wingborg, N., Nilsson, C., 2014. Green space propulsion: Opportunities and prospects. Progress in Aerospace Sciences 71, 128–149. https://doi.org/10.1016/j.paerosci.2014.08.001

Graham, E.B., Knelman, J.E., Schindlbacher, A., Siciliano, S., Breulmann, M., Yannarell, A., Beman, J.M., Abell, G., Philippot, L., Prosser, J., Foulquier, A., Yuste, J.C., Glanville,

H.C., Jones, D.L., Angel, R., Salminen, J., Newton, R.J., Bürgmann, H., Ingram, L.J., Hamer, U., Siljanen, H.M.P., Peltoniemi, K., Potthast, K., Bañeras, L., Hartmann, M., Banerjee, S., Yu, R.-Q., Nogaro, G., Richter, A., Koranda, M., Castle, S.C., Goberna, M., Song, B., Chatterjee, A., Nunes, O.C., Lopes, A.R., Cao, Y., Kaisermann, A., Hallin, S., Strickland, M.S., Garcia-Pausas, J., Barba, J., Kang, H., Isobe, K., Papaspyrou, S., Pastorelli, R., Lagomarsino, A., Lindström, E.S., Basiliko, N., Nemergut, D.R., 2016. Microbes as Engines of Ecosystem Function: When Does Community Structure Enhance Predictions of Ecosystem Processes? Front. Microbiol. 7. https://doi.org/10.3389/fmicb.2016.00214

Gujer, W., Henze, M., Mino, T., van Loosdrecht, M., 1999. Activated Sludge Model No. 3. Water Science and Technology 39, 183–193. https://doi.org/10.2166/wst.1999.0039

Henze, M., Gujer, W., Mino, T., Matsuo, T., Wentzel, M.C., Marais, G. v. R., Van Loosdrecht, M.C.M., 1999. Activated Sludge Model No.2d, ASM2D. Water Science and Technology 39, 165–182. https://doi.org/10.2166/wst.1999.0036

Hu, Z., Zhang, J., Xie, H., Li, S., Wang, J., Zhang, T., 2011. Effect of anoxic/aerobic phase fraction on N2O emission in a sequencing batch reactor under low temperature. Bioresource Technology 102, 5486–5491. https://doi.org/10.1016/j.biortech.2010.10.037

Kelly, J., 2016. The First Drag Racers to Ever Use Nitrous Oxide. MotorTrend.

Le Vaillant, F., Mateos Calbet, A., González-Pelayo, S., Reijerse, E.J., Ni, S., Busch, J., Cornella, J., 2022. Catalytic synthesis of phenols with nitrous oxide. Nature 604, 677–683. https://doi.org/10.1038/s41586-022-04516-4

Liu, Y., Peng, L., Chen, X., Ni, B.-J., 2015a. Mathematical Modeling of Nitrous Oxide Production during Denitrifying Phosphorus Removal Process. Environ. Sci. Technol. 49, 8595–8601. https://doi.org/10.1021/acs.est.5b01650

Liu, Y., Peng, L., Guo, J., Chen, X., Yuan, Z., Ni, B.-J., 2015b. Evaluating the Role of Microbial Internal Storage Turnover on Nitrous Oxide Accumulation During Denitrification. Sci Rep 5, 15138. https://doi.org/10.1038/srep15138

Lv, X., Shao, M., Li, C., Li, J., Liu, D., Gao, X., Xia, X., 2014. Operation performance and microbial community dynamics of phosphorus removal sludge with different electron acceptors. Journal of Industrial Microbiology and Biotechnology 41, 1099–1108. https://doi.org/10.1007/s10295-014-1444-1

Marques, R., Ribera-Guardia, A., Santos, J., Carvalho, G., Reis, M.A.M., Pijuan, M., Oehmen, A., 2018. Denitrifying capabilities of Tetrasphaera and their contribution towards nitrous oxide production in enhanced biological phosphorus removal processes. Water Research 137, 262–272. https://doi.org/10.1016/j.watres.2018.03.010

McIlroy, S.J., Albertsen, M., Andresen, E.K., Saunders, A.M., Kristiansen, R., Stokholm-Bjerregaard, M., Nielsen, K.L., Nielsen, P.H., 2014. 'Candidatus Competibacter'-lineage genomes retrieved from metagenomes reveal functional metabolic diversity. ISME J 8, 613–624. https://doi.org/10.1038/ismej.2013.162

McIlroy, S.J., Onetto, C.A., McIlroy, B., Herbst, F.-A., Dueholm, M.S., Kirkegaard, R.H., Fernando, E., Karst, S.M., Nierychlo, M., Kristensen, J.M., Eales, K.L., Grbin, P.R., Wimmer, R., Nielsen, P.H., 2018. Genomic and in Situ Analyses Reveal the Micropruina spp. as Abundant Fermentative Glycogen Accumulating Organisms in Enhanced Biological Phosphorus Removal Systems. Front. Microbiol. 9, 1004. https://doi.org/10.3389/fmicb.2018.01004

Nadeau, S.A., Roco, C.A., Debenport, S.J., Anderson, T.R., Hofmeister, K.L., Walter, M.T., Shapleigh, J.P., 2019. Metagenomic analysis reveals distinct patterns of denitrification gene abundance across soil moisture, nitrate gradients. Environmental Microbiology 21, 1255–1266. https://doi.org/10.1111/1462-2920.14587

Oehmen, A., Lopez-Vazquez, C.M., Carvalho, G., Reis, M.A.M., Van Loosdrecht, M.C.M., 2010. Modelling the population dynamics and metabolic diversity of organisms relevant in anaerobic/anoxic/aerobic enhanced biological phosphorus removal processes. Water Research 44, 4473–4486. https://doi.org/10.1016/j.watres.2010.06.017

Oehmen, A., Yuan, Z., Blackall, L.L., Keller, J., 2005. Comparison of acetate and propionate uptake by polyphosphate accumulating organisms and glycogen accumulating organisms. Biotech & Bioengineering 91, 162–168. https://doi.org/10.1002/bit.20500

Parada, A.E., Needham, D.M., Fuhrman, J.A., 2016. Every base matters: assessing small subunit rRNA primers for marine microbiomes with mock communities, time series and global field samples: Primers for marine microbiome studies. Environ Microbiol 18, 1403–1414. https://doi.org/10.1111/1462-2920.13023

Peng, L., Ni, B.-J., Ye, L., Yuan, Z., 2015. The combined effect of dissolved oxygen and nitrite on N2O production by ammonia oxidizing bacteria in an enriched nitrifying sludge. Water Research 73, 29–36. https://doi.org/10.1016/j.watres.2015.01.021

Petriglieri, F., Singleton, C.M., Kondrotaite, Z., Dueholm, M.K.D., McDaniel, E.A., McMahon, K.D., Nielsen, P.H., 2022. Reevaluation of the Phylogenetic Diversity and Global Distribution of the Genus " *Candidatus* Accumulibacter." mSystems e00016-22. https://doi.org/10.1128/msystems.00016-22

Reichert, P., 1994. AQUASIM-A tool for simulation and data analysis of aquatic systems. Water Science and Technology 30, 21.

Ren, S., Liu, Yingrui, He, Y., Zhu, T., Chen, X., Liu, Yiwen, 2023. Mathematical modeling of the dynamic effect of denitrifying glycogen-accumulating organisms on nitrous oxide production during denitrifying phosphorus removal. Chemical Engineering Journal 453, 139802. https://doi.org/10.1016/j.cej.2022.139802

Ribera-Guardia, A., Marques, R., Arangio, C., Carvalheira, M., Oehmen, A., Pijuan, M., 2016. Distinctive denitrifying capabilities lead to differences in N2O production by denitrifying polyphosphate accumulating organisms and denitrifying glycogen accumulating organisms. Bioresource Technology 219, 106–113. https://doi.org/10.1016/j.biortech.2016.07.092

Roots, P., Sabba, F., Rosenthal, A.F., Wang, Y., Yuan, Q., Rieger, L., Yang, F., Kozak, J.A., Zhang, H., Wells, G.F., 2020. Integrated shortcut nitrogen and biological phosphorus removal from mainstream wastewater: process operation and modeling. Environ. Sci.: Water Res. Technol. 6, 566–580. https://doi.org/10.1039/C9EW00550A

Sampara, P., Luo, Y., Lin, X., Ziels, R.M., 2022. Integrating Genome-Resolved Metagenomics with Trait-Based Process Modeling to Determine Biokinetics of Distinct Nitrifying Communities within Activated Sludge. Environ. Sci. Technol. 56, 11670–11682. https://doi.org/10.1021/acs.est.2c02081

Scherson, Y.D., Wells, G.F., Woo, S.-G., Lee, J., Park, J., Cantwell, B.J., Criddle, C.S., 2013. Nitrogen removal with energy recovery through $N_2O$ decomposition. Energy Environ. Sci. 6, 241–248. https://doi.org/10.1039/C2EE22487A

Scherson, Y.D., Woo, S.-G., Criddle, C.S., 2014. Production of Nitrous Oxide From Anaerobic Digester Centrate and Its Use as a Co-oxidant of Biogas to Enhance Energy Recovery. Environ. Sci. Technol. 48, 5612–5619. https://doi.org/10.1021/es501009j

Shao, X., Zhao, L., Sheng, X., Wu, M., 2020. Effects of influent salinity on water purification and greenhouse gas emissions in lab-scale constructed wetlands. Environ Sci Pollut Res 27, 21487–21496. https://doi.org/10.1007/s11356-020-08497-7

Smith, C., Hill, A.K., Torrente-Murciano, L., 2020. Current and future role of Haber–Bosch ammonia in a carbon-free energy landscape. Energy Environ. Sci. 13, 331–344. https://doi.org/10.1039/C9EE02873K

Stewart, R.D., Myers, K.S., Amstadt, C., Seib, M., McMahon, K.D., Noguera, D.R., 2024. Refinement of the " *Candidatus* Accumulibacter" genus based on metagenomic analysis of biological nutrient removal (BNR) pilot-scale plants operated with reduced aeration. mSystems 9, e01188-23. https://doi.org/10.1128/msystems.01188-23

Su, X., Zhu, X., Li, J., Wu, L., Li, X., Zhang, Q., Peng, Y., 2023. Determination of partial denitrification kinetic model parameters based on batch tests and metagenomic sequencing. Bioresource Technology 379, 128977. https://doi.org/10.1016/j.biortech.2023.128977

Tamis, J., Lužkov, K., Jiang, Y., Loosdrecht, M.C.M.V., Kleerebezem, R., 2014. Enrichment of Plasticicumulans acidivorans at pilot-scale for PHA production on industrial wastewater. Journal of Biotechnology 192, 161–169. https://doi.org/10.1016/j.jbiotec.2014.10.022

Tayà, C., Garlapati, V.K., Guisasola, A., Baeza, J.A., 2013. The selective role of nitrite in the PAO/GAO competition. Chemosphere 93, 612–618. https://doi.org/10.1016/j.chemosphere.2013.06.006

Vasilaki, V., Massara, T.M., Stanchev, P., Fatone, F., Katsou, E., 2019. A decade of nitrous oxide (N2O) monitoring in full-scale wastewater treatment processes: A critical review. Water Research 161, 392–412. https://doi.org/10.1016/j.watres.2019.04.022

Velho, V.F., Magnus, B.S., Daudt, G.C., Xavier, J.A., Guimarães, L.B., Costa, R.H.R., 2017. Effect of COD/N ratio on N2O production during nitrogen removal by aerobic granular sludge. Water Science and Technology 76, 3452–3460. https://doi.org/10.2166/wst.2017.502

Vieira, A., Ribera-Guardia, A., Marques, R., Barreto Crespo, M.T., Oehmen, A., Carvalho, G., 2018. The link between the microbial ecology, gene expression, and biokinetics of denitrifying polyphosphate-accumulating systems under different electron acceptor combinations. Appl Microbiol Biotechnol 102, 6725–6737. https://doi.org/10.1007/s00253-018-9077-3

Wang, X., Zhang, G., Ding, A., Xie, E., Tan, Q., Xing, Y., Wu, H., Tian, Q., Zhang, Y., Zheng, L., 2024. Distinctive species interaction patterns under high nitrite stress shape inefficient denitrifying phosphorus removal performance. Bioresource Technology 394, 130269. https://doi.org/10.1016/j.biortech.2023.130269

Wang, Y., Gao, H., Wells, G., 2021. Integrated omics analyses reveal differential gene expression and potential for cooperation between denitrifying polyphosphate and glycogen accumulating organisms. Environ Microbiol 23, 3274–3293. https://doi.org/10.1111/1462-2920.15486

Wang, Z., Woo, S.-G., Yao, Y., Cheng, H.-H., Wu, Y.-J., Criddle, C.S., 2020. Nitrogen removal as nitrous oxide for energy recovery: Increased process stability and high nitrous yields at

short hydraulic residence times. Water Research 173, 115575. https://doi.org/10.1016/j.watres.2020.115575

Weißbach, M., Thiel, P., Drewes, J.E., Koch, K., 2018. Nitrogen removal and intentional nitrous oxide production from reject water in a coupled nitritation/nitrous denitritation system under real feed-stream conditions. Bioresource Technology 255, 58–66. https://doi.org/10.1016/j.biortech.2018.01.080

Werling, L.K., Hörger, T., Manassis, K., Grimmeisen, D., Wilhelm, M., Erdmann, C., Ciezki, H.K., Schlechtriem, S., Richter, S., Torsten, M., others, 2020. Nitrous oxide fuels blends: research on premixed monopropellants at the german aerospace center (DLR) since 2014, in: AIAA Propulsion and Energy 2020 Forum. p. 3807.

Zeng, R.J., Lemaire, R., Yuan, Z., Keller, J., 2003. Simultaneous nitrification, denitrification, and phosphorus removal in a lab□scale sequencing batch reactor. Biotech & Bioengineering 84, 170–178. https://doi.org/10.1002/bit.10744

Ziliani, A., Bovio-Winkler, P., Cabezas, A., Etchebehere, C., Garcia, H.A., López-Vázquez, C.M., Brdjanovic, D., van Loosdrecht, M.C.M., Rubio-Rincón, F.J., 2023. Putative metabolism of Ca. Accumulibacter via the utilization of glucose. Water Research 229, 119446. https://doi.org/10.1016/j.watres.2022.119446